

## DAMAGE IDENTIFICATION IN BEAM-LIKE STRUCTURE USING RELATIVE NATURAL FREQUENCY SHIFTS

Duc Tuan Ta<sup>1,\*</sup>, Van Tuan Vu<sup>1</sup>

<sup>1</sup>*Institute of Techniques for Special Engineering, Le Quy Don Technical University*

### Abstract

Vibration-based damage identification methods have demonstrated significant potential for structural health monitoring. Modal parameters, including natural frequencies and mode shapes, serve as global indicators of a structure's condition. Changes in these parameters can be indicative of damage within the structure. This article proposes an enhanced methodology for damage detection through shifts in natural frequencies. By precisely determining the frequencies of both the intact and damaged structure, frequency shifts can be computed, thereby transforming the damage detection process into a minimization of error in the identification task. This approach involves comparing the measured frequency variations with analytical values, which characterizes the frequency shifts resulting from damage. The effectiveness of the proposed procedure is validated through numerical simulations, followed by experimental testing.

**Keywords:** *Damage detection; natural frequency shift; mode shapes.*

### 1. Introduction

Structural damage detection is crucial, particularly in the early stages, to prevent sudden failures and enhance the safety and longevity of structures [1]. Vibration-based fault detection methods, which rely on monitoring changes in dynamic properties such as natural frequencies, mode shapes, and damping ratios, have shown significant potential in mechanical systems [2], [3]. These methods are particularly advantageous in practical applications, especially when operational modal analysis is employed, as they enable continuous monitoring without disrupting the regular operation of structures.

Numerous studies have employed these dynamic parameters for damage identification. Y. S. Lee and M. J. Chung [4] applied Armon's rank ordering method to estimate the crack location in a cantilever beam, using the first four natural frequencies of the damaged structure. D. P. Patil and S. K. Maiti [5] proposed a crack detection method based on a rotational spring model to simulate the crack effect in a beam, with the damage index representing the strain energy stored in the spring. G. R. Gillich *et al.* [6] suggested comparing measured frequency changes with analytically derived values and employing pattern recognition techniques to determine the damage location and severity. M. Dahak

---

\* Corresponding author, email: tuantd@lqdtu.edu.vn  
DOI: 10.56651/lqdtu.jst.v8.n2.965.sce

*et al.* [7] focused on using normalized natural frequencies to identify damage in a cantilever beam. Sha *et al.* [8] combined relative natural frequency variations and measured data with Bayesian inference for damage detection. C. Surace *et al.* [9] used frequency ratio comparisons across different modes as indicators for damage characteristics.

Changes in mode shapes and modal curvatures have also been extensively studied for damage detection. Mode shapes directly provide information about damage location [10], and differences in modal curvatures between intact and damaged states can be used to localize damage [11], [12]. R. Gorgin [13] developed a method for damage localization based on the analysis of the first mode shape. However, these methods typically require extensive measurements at multiple locations and are often limited to damage localization.

To overcome these limitations, combined methods that integrate natural frequencies and mode shapes (or their derivatives) have been proposed for more comprehensive damage quantification. M. Dahak *et al.* [14] introduced a method that uses the intersection of curves derived from the curvature of the intact mode shape and measured frequencies. The use of the relationship between natural frequency shifts and modal curvatures for damage detection was also explored in [15].

Recent advancements in computational power and sensor technology have facilitated the application of machine learning techniques in damage detection [16]-[19]. While effective, these techniques often require significant computational resources, making them time-intensive.

This study focuses on rapid damage identification methods, particularly effective during the early stages of damage detection in beam-like structures. Among the methods discussed, those that use natural frequency shifts and analytical modal curvatures are particularly effective for detecting single cracks in beams [6], [14], [15]. The proposed method involves generating curves based on relative natural frequency shifts and modal curvatures along the beam's length. The intersection of these curves is then used for damage localization. However, the intersection is not always obvious, complicating the identification process. To address this challenge, an improved procedure is presented that uses singular value decomposition technique to highlight the intersection, thus simplifying the damage location identification. The proposed method is validated through numerical simulations and experimental tests.

## 2. Vibration analysis

Consider an Euler-Bernoulli beam with the following equation of motion:

$$\frac{\partial^4 y(x,t)}{\partial x^4} + \frac{\rho A}{EI} \frac{\partial^2 y(x,t)}{\partial x^2} = 0 \quad (1)$$

where  $y(x,t)$  is the vertical displacement of the beam at a coordinate  $x$  and time  $t$ ;  $E$ ,  $\rho$  are Young's modulus and the density of the beam material;  $I$ ,  $A$  are the inertia moment and the area of the cross-section of the beam, respectively.

The root of the above equation can be represented:

$$y(x,t) = \phi(x) \sin(\omega t + \varphi) \quad (2)$$

where  $\phi(x)$ ,  $\omega$  and  $\varphi$  are the mode shape, the angular frequency, and the phase shift, respectively.

The mode shape  $\phi(x)$  is represented by the following form:

$$\phi(x) = a_1 \sin(\alpha x) + a_2 \cos(\alpha x) + a_3 \sinh(\alpha x) + a_4 \cosh(\alpha x) \quad (3)$$

in which

$$\alpha = \sqrt{\frac{\rho A \omega^2}{EI}} \quad (4)$$

The second derivative (modal curvature) of the mode shape has the following form:

$$\phi''(x) = \alpha^2 (-a_1 \sin(\alpha x) - a_2 \cos(\alpha x) + a_3 \sinh(\alpha x) + a_4 \cosh(\alpha x)) \quad (5)$$

## 2.1. Cantilever beam

Apply the boundary condition of the cantilever beam with  $\phi(0) = 0$ ,  $\phi'(0) = 0$ ,  $\phi''(L) = 0$ ,  $\phi'''(L) = 0$  where  $a_1$ ,  $a_2$ ,  $a_3$ , and  $a_4$  can be obtained as follows:

$$a_1 = -a_3; a_2 = -a_4; a_1 = -a_2 \frac{\cos(\alpha L) + \cosh(\alpha L)}{\sin(\alpha L) + \sinh(\alpha L)} \quad (6)$$

The values  $\alpha$  for modes can be determined from the following characteristic equation:

$$1 + \cos(\alpha L) \cosh(\alpha L) = 0 \quad (7)$$

The mode shapes and modal curvature of a cantilever beam are shown in Fig. 1.

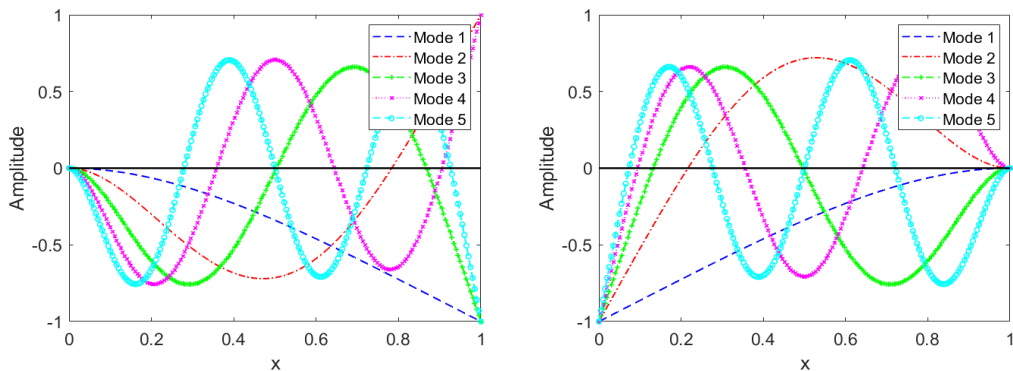


Fig. 1. Mode shapes (left) and modal curvature (right) of a cantilever beam.

## 2.2. Clamped-clamped beam (2-ends fully fixed beam)

Apply the boundary condition of the fully fixed-fixed beam with  $\phi(0) = 0, \phi(L) = 0, \phi'(0) = 0, \phi'(L) = 0$  where  $a_1, a_2, a_3$  and  $a_4$  are obtained as follows:

$$a_1 = -a_3; a_2 = -a_4; a_1 = a_2 \frac{\cos(\alpha L) - \cosh(\alpha L)}{\sin(\alpha L) - \sinh(\alpha L)} \quad (8)$$

The values  $\alpha$  for modes can be determined from the following characteristic equation:

$$1 - \cos(\alpha L) \cosh(\alpha L) = 0 \quad (9)$$

Figure 2 shows the mode shapes and modal curvature of a fixed-fixed beam.

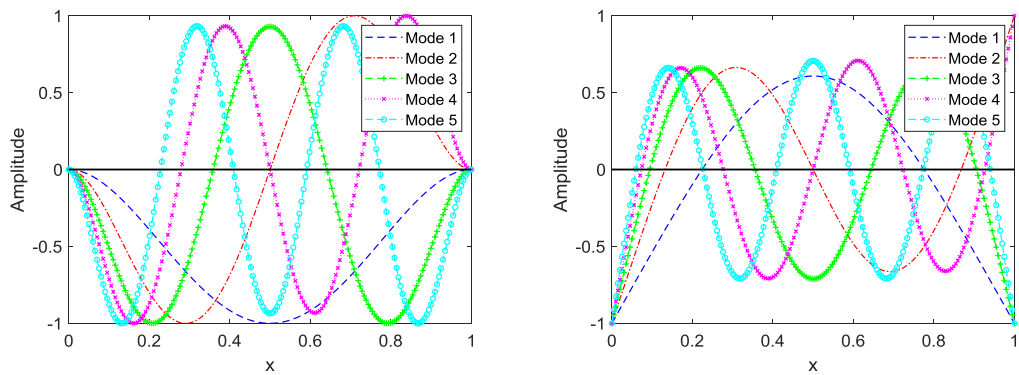


Fig. 2. Mode shapes (left) and modal curvature (right) of a fully fixed-fixed beam.

## 2.3. Damage analysis

The relationship between relative natural frequency shift and damage at location  $x_0$  is obtained as [20]:

$$\overline{\Delta f_i} = \frac{\Delta f_i}{f_i} = \frac{f_i - \overline{f_i}}{f_i} \approx \delta_K \frac{\phi_i''(x_0)}{\|\phi_i''\|_2^2} + \delta_M \frac{\phi_i^2(x_0)}{\|\phi_i\|_2^2} \quad (10)$$

where  $f_i$  and  $\overline{f_i}$  are the natural frequencies of the  $i^{th}$  mode of the intact and damaged states, respectively;  $\delta_K = \frac{\Delta EI \Delta L}{2EI}$  and  $\delta_M = -\frac{\Delta \mu \Delta L}{2\mu}$  are the relative local variation of bending stiffness and mass, respectively;  $\phi_i$  and  $\phi_i''$  are the intact mode shape and the intact modal curvature of the  $i^{th}$  mode.

In the case of damage due only to a change in bending stiffness and neglecting the effect of mass changes, a simplified expression for the relative natural frequency variation can be expressed as a function of the squared modal curvature [6], [8]:

$$\overline{\Delta f_i} = \zeta \phi_i''^2(x_0) \quad (11)$$

where  $\zeta$  represents the damage coefficient and depends on the severity of the damage.

The damage coefficient can be expressed by the relative change in natural frequency as follows:

$$\zeta \approx \frac{\overline{\Delta f_i}}{\phi_i''^2(x_0)} \quad (12)$$

Each damage coefficient  $\zeta$  is a constant for all modes. Therefore, the damage location  $x_0$  can be determined by the mutual intersection of the curves obtained from the intact modal curvature and the relative natural frequency shift of the modes.

### 3. Damage detection technique

To accurately calculate the position of the mutual intersection of these curves, a approach based on singular value decomposition (SVD) technique is proposed as follows:

- Divide the length of the beam into  $n$  positions. For each mode  $i$  at each location  $x_j$  one gets:

$$\zeta_{i,j} \approx \frac{\overline{\Delta f_i}}{\phi_i''^2(x_j)} \text{ with } i = 1:m \text{ and } j = 1:n \text{ with } m \ll n \text{ where } m \text{ is the number of modes.}$$

- Define the following matrix  $A^{(j)}$  for each location  $x_j$ :

$$A_{(m+1) \times m}^{(j)} = \begin{bmatrix} 1 & 1 & \dots & 1 & \dots & 1 \\ \zeta_{1,j} & \zeta_{2,j} & \dots & \zeta_{i,j} & \dots & \zeta_{m,j} \\ \zeta_{1,j} & \zeta_{1,j} & \dots & \zeta_{1,j} & \dots & \zeta_{1,j} \\ \zeta_{1,j} & \zeta_{2,j} & \dots & \zeta_{i,j} & \dots & \zeta_{m,j} \\ \zeta_{2,j} & \zeta_{2,j} & \dots & \zeta_{2,j} & \dots & \zeta_{2,j} \\ \vdots & \vdots & \dots & \vdots & \dots & \vdots \\ \zeta_{1,j} & \zeta_{2,j} & \dots & \zeta_{i,j} & \dots & \zeta_{m,j} \\ \zeta_{i,j} & \zeta_{i,j} & \dots & \zeta_{i,j} & \dots & \zeta_{i,j} \\ \vdots & \vdots & \dots & \vdots & \dots & \vdots \\ \zeta_{1,j} & \zeta_{2,j} & \dots & \zeta_{i,j} & \dots & \zeta_{m,j} \\ \zeta_{m,j} & \zeta_{m,j} & \dots & \zeta_{m,j} & \dots & \zeta_{m,j} \end{bmatrix} \quad (13)$$

- Take a singular value decomposition of matrix  $A^{(j)}$  to obtain  $m$  singular values

for each location  $x_j$ :

$$s_1^{(j)} > s_2^{(j)} > \dots > s_m^{(j)} > 0 \quad (14)$$

When  $x \rightarrow x_0$ , all elements in matrix  $A^{(j)}$  tend to be 1, and thus:

$$s_1^{(j)} > 0 \text{ and } s_2^{(j)}, s_3^{(j)}, \dots, s_m^{(j)} \rightarrow 0 \quad (15)$$

- Plot the curve  $p(x_j) = \frac{1}{s_2^{(j)}}$  over the length of the beam. Then, the peak at location  $x = x_0$  is observed.

Summarizing the above analysis, Figure 3 presents a schematic diagram outlining the process of identifying single damage in beam-like structures.

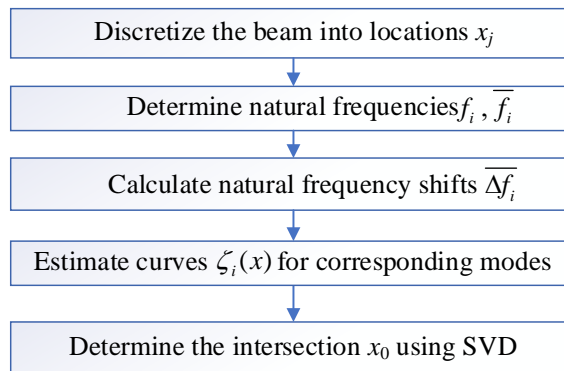


Fig. 3. Flowchart for damage identification.

Discretizing the beam into smaller segments in the first step, this can achieve a higher level of detail in the analysis. This leads to more accurate results, particularly in regions where the intersection of curves may happen.

#### 4. Numerical tests

This section aims to provide a comprehensive assessment of the beam's integrity and the efficacy of the proposed method for evaluating structural damage. The validation of the proposed procedure is conducted through the analysis of a structural model simulated in ANSYS Workbench. The numerical investigations focus on a steel beam characterized by a Young's modulus of 200 GPa and a mass density of 7850 kg/m<sup>3</sup>. The beam, with dimensions of 800 mm in length, 40 mm in width, and 6 mm in height, is subjected to various boundary conditions to assess its structural response. All simulated imperfections are represented as damage sites of 2 mm in width.

##### 4.1. Cantilever beam

In the context of a numerical cantilever beam analysis, exploring various damage

scenarios is crucial for understanding the beam's structural integrity under different damage locations. The model is presented in Fig. 4. Three damage cases are considered, differing in crack location and depth (see Tab. 1). Following the proposed procedure, the intersection point is determined to represent the damage location as shown in Figs. 5-7. The results are presented in Tab. 2.

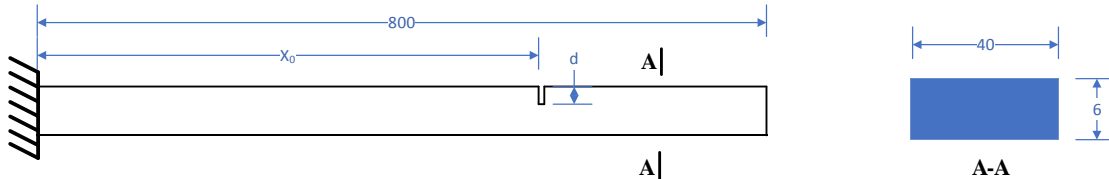


Fig. 4. A cantilever beam.

Tab. 1. Damage scenarios of the numerical cantilever beam

Case	Damage		Natural frequency (Hz)			
	$x_0$ (cm)	d (cm)	Mode 1	Mode 2	Mode 3	Mode 4
Intact	0	0	7.6850	48.149	134.79	264.08
1	20	1.0	7.6447	48.145	134.33	263.03
2	30	1.5	7.6629	47.579	134.77	261.06
3	60	2.0	7.682	47.753	131.69	258.98

Tab. 2. Results estimated from the numerical tests

No.	Exact damage location (cm)	Identified damage location (cm)	Error (%)
1	20	19.54	2.3
2	30	29.79	0.7
3	60	59.51	0.8

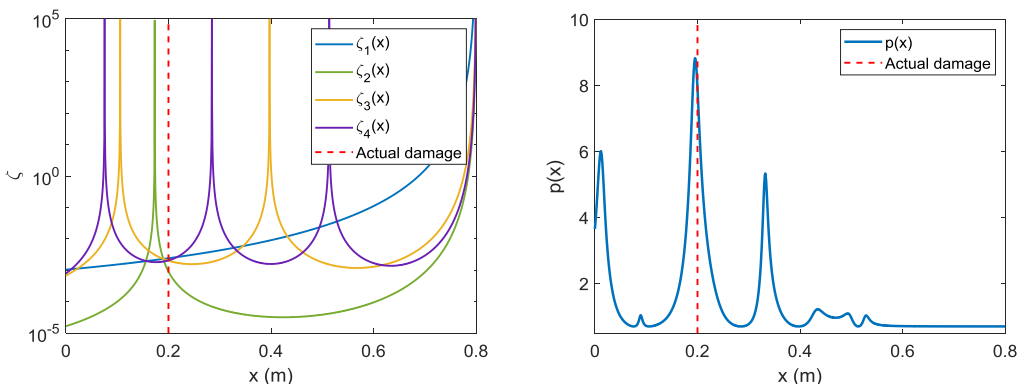


Fig. 5. Curves and identified damage location for case 1 (cantilever beam).

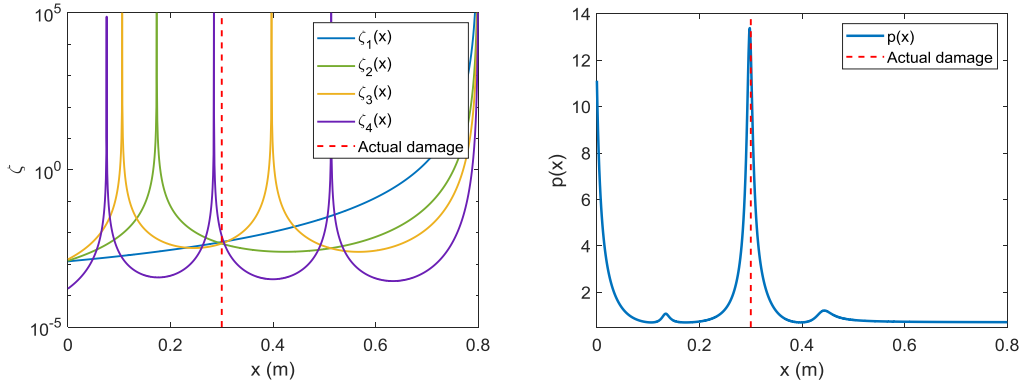


Fig. 6. Curves and identified damage location for case 2 (cantilever beam).

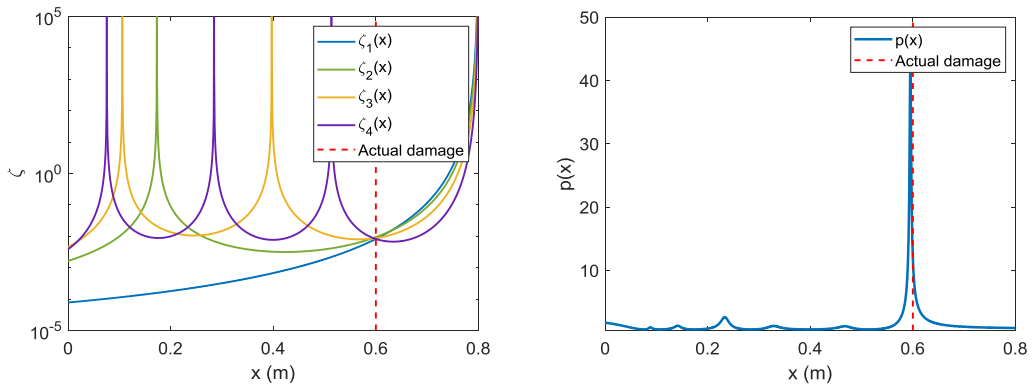


Fig. 7. Curves and identified damage location for case 3 (cantilever beam).

#### 4.2. Fixed-fixed beam

In this section, a fixed-fixed beam model is studied as shown in Fig. 8. Three damage cases are considered, differing in crack location and depth (see Tab. 3). Following the proposed procedure, the intersection point is determined to represent the damage location as shown in Figs. 9-11. The estimated results are presented in Tab. 4.

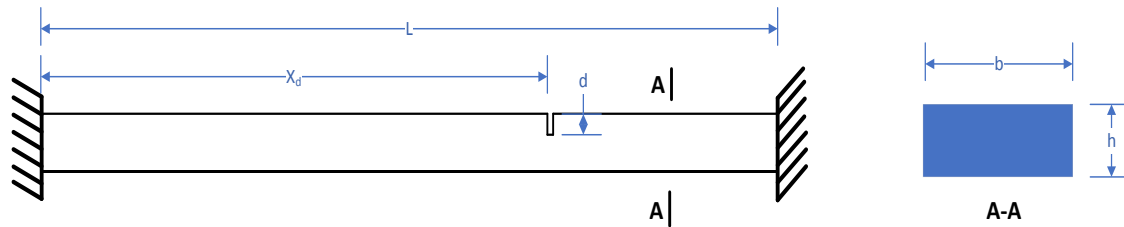


Fig. 8. A fixed-fixed beam.

Tab. 3. Damage scenarios of the numerical fixed-fixed beam

Case	Damage		Natural frequency (Hz)			
	$x_0$ (cm)	d (cm)	Mode 1	Mode 2	Mode 3	Mode 4
Intact	0	0	49.142	135.41	265.35	438.47
1	15	1.0	49.125	135.26	264.36	436.64
2	20	1.5	49.131	134.36	263.06	437.68
3	35	2.0	48.491	134.79	261.9	433.15

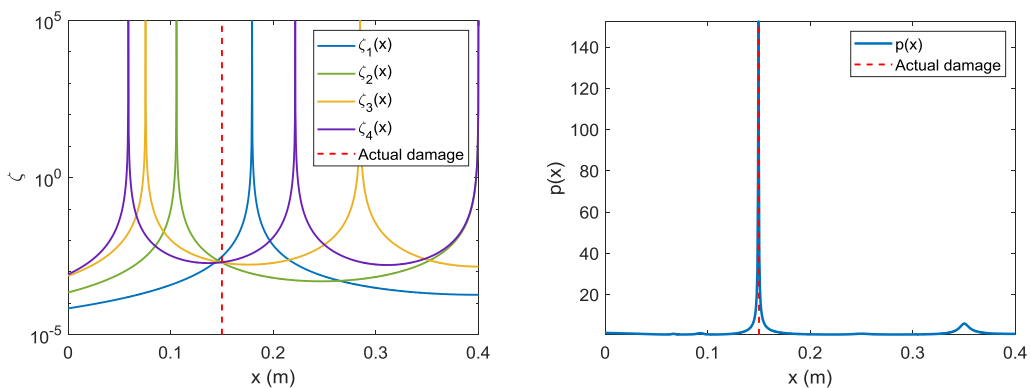


Fig. 9. Curves and identified damage location for case 1 (fixed-fixed beam).

Tab. 4. Results estimated from the numerical tests

No.	Actual damage location (cm)	Identified damage location (cm)	Error (%)
1	15	14.94	0.3
2	20	19.78	1.1
3	35	35.09	0.3

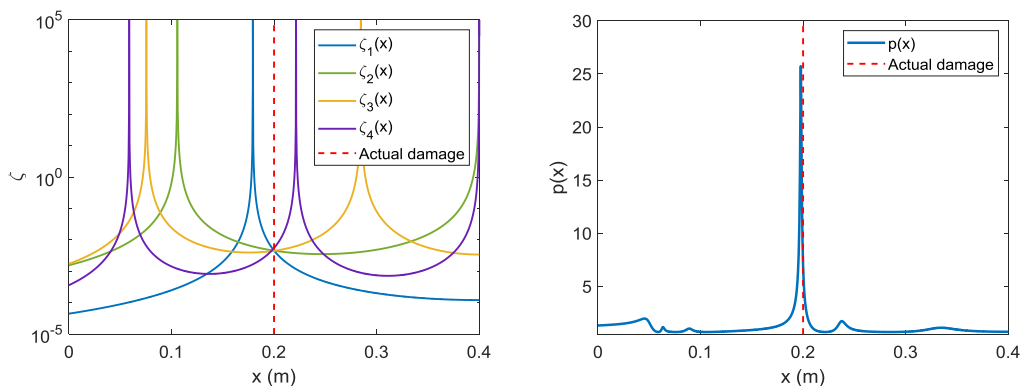


Fig. 10. Curves and identified damage location for case 2 (fixed-fixed beam).

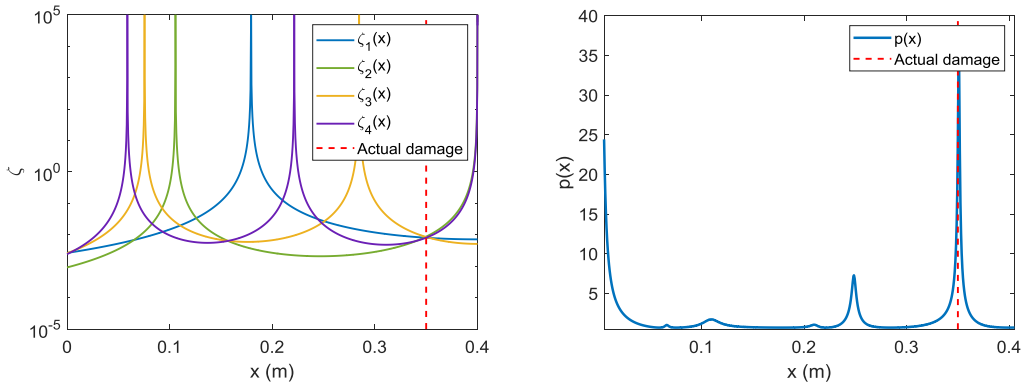


Fig. 11. Curves and identified damage location for case 3 (fixed-fixed beam).

## 5. Experimental validation

The physical dimensions of beams used in experimental studies can be chosen randomly. In this experiment, a readily available beam was used to conduct the experimental research. It has the following physical parameters: length  $L = 1005$  mm, width  $B = 42$  mm and height  $H = 10$  mm. The material of the beam has Young's modulus  $E = 200$  GPa and density  $= 7850$  kg/m<sup>3</sup>.

In this work, a cut 2 mm wide and 5 mm deep is made by machining. It is located at a distance of 220 mm from the support. The five accelerometers were placed at different locations on the beam to capture responses (as shown in Fig. 12). Once the time response was collected, the Rational Fraction Polynomial (RFP) method in B&K Connect™ was used to convert the time domain data into the frequency domain. This helps determine the natural frequency of the beam. The natural frequencies of the intact beam were measured first. These frequencies served as a baseline for understanding the structural integrity of the beam. After introducing a damage scenario, modal testing was repeated to determine the new natural frequencies. The damage leads to lower natural frequencies due to a reduction in stiffness (Tab. 5). The identified location of the damage is shown in Fig. 13. The identified results are presented in Tab. 6. They are close to real values which confirms the proposed method.

Tab. 5. Frequencies of the experimental test for the cantilever beam

No.	Damage	Natural frequency (Hz)			
		$x_0$ (cm)	Mode 1	Mode 2	Mode 3
Intact	0		7.769	48.366	137.350
Damage	22.0		7.767	48.365	137.339
					277.269
					277.240

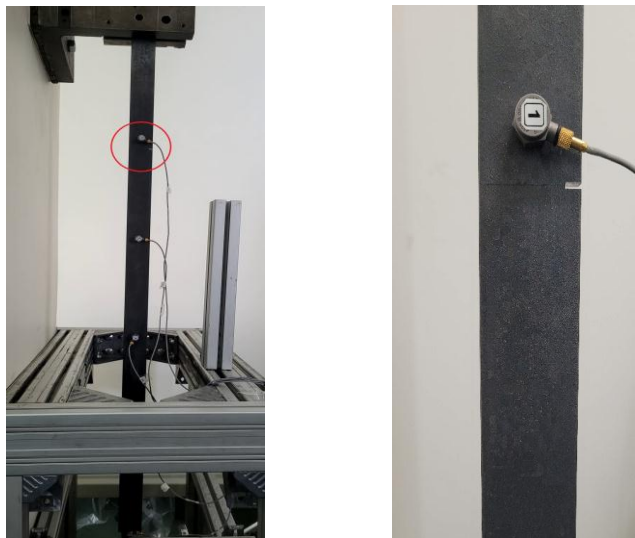


Fig. 12. A whole system view (left) and damage area (right) of the test.

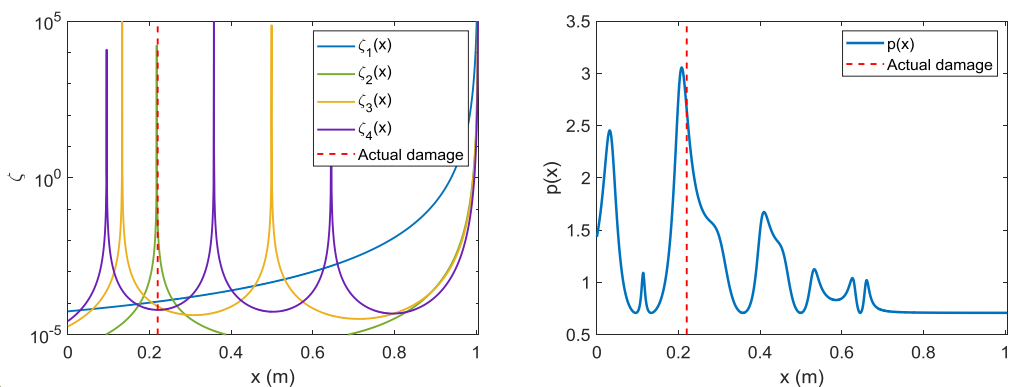


Fig. 13. Damage detection for the experimental test.

Tab. 6. Results estimated from the experimental test

No.	Actual damage location (cm)	Identified damage location (cm)	Error (%)
1	22.0	20.8	5.4

The size of the crack can affect the detection capability of the proposed method. Generally, very small cracks are more challenging to detect because they may produce less distinguishable changes compared to larger cracks.

Besides, this method requires at least three modes to obtain accurate results. Using more vibration modes can enhance damage detection accuracy in structural health monitoring. Effective identification requires careful measurement and analysis techniques to estimate the multiple modes of the structure.

## 6. Conclusion

This study presents an innovative approach for detecting localized damage in beam-like structures. The method begins with the construction of damage coefficient curves along the length of the beam, which are derived from shifts in relative natural frequencies and analytical modal curvatures. The location of the damage is identified by precisely determining the intersection point of these coefficient curves. To ensure accurate localization of this intersection, the procedure utilizes a numerical technique based on Singular Value Decomposition (SVD) applied to matrices constructed from the ratios of the damage coefficient curves. The proposed method was first validated through numerical simulations on cantilever and fixed-fixed beam models, demonstrating high accuracy in identifying the damage location when compared to the known damage conditions. Finally, the method was experimentally tested on a cantilever beam, where the results of damage detection closely matched the actual damage, thus confirming the effectiveness and reliability of the proposed approach for detecting localized damage in beam-like structures.

In the case of multiple cracks in a structure, the effects of multiple cracks are assumed to follow the superposition principle. If each crack is independent, then the individual effects will be added together. This identification process requires additional steps, which will be published in future work.

## References

- [1] H. P. Chen and Y. Q. Ni. *Structural Health Monitoring of Large Civil Engineering Structures*, John Wiley & Sons Ltd., UK, 2018.
- [2] S. W. Doebling, C. Farrar, M. B. Prime, and D. W. Shevitz, “Damage identification and health monitoring of structural and mechanical systems from changes in their vibration characteristics: A literature review”, *The Shock and Vibration Digest*, Vol. 30, 1996. DOI: 10.2172/249299
- [3] O. Avci *et al.*, “A review of vibration-based damage detection in civil structures: From traditional methods to machine learning and deep learning applications”, *Mechanical Systems and Signal Processing*, Vol. 147, 2021. DOI: 10.1016/j.ymssp.2020.107077
- [4] Y. S. Lee and M. J. Chung, “A study on crack detection using eigenfrequency test data”, *Computers & Structures*, Vol. 77, Iss. 3, pp. 327-342, 2000. DOI: 10.1016/S0045-7949(99)00194-7
- [5] D. P. Patil and S. K. Maiti, “Experimental verification of a method of detection of multiple cracks in beams based on frequency measurements”, *Journal of Sound and Vibration*, Vol. 281, pp. 439-451, 2005. DOI: 10.1016/j.jsv.2004.03.035

- [6] G. R. Gillich and Z. I. Praisach, "Modal identification and damage detection in beam-like structures using the power spectrum and time-frequency analysis", *Signal Processing*, Vol. 96, pp. 29-44, 2014. DOI: 10.1016/j.sigpro.2013.04.027
- [7] M. Dahak, N. Touat, and N. Benseddiq, "On the classification of normalized natural frequencies for damage detection in cantilever beam", *Journal of Sound and Vibration*, Vol. 402, pp. 70-84. 2017. DOI: 10.1016/j.jsv.2017.05.007
- [8] G. Sha, M. Radzienski, M. Cao, and W. Ostachowicz, "A novel method for single and multiple damage detection in beams using relative natural frequency changes", *Mechanical Systems and Signal Processing*, Vol. 132, pp. 335-352, 2019. DOI: 10.1016/j.ymssp.2019.06.027
- [9] C. Surace and A. Bovsunovskii, "The use of frequency ratios to diagnose structural damage in varying environmental conditions", *Mechanical Systems and Signal Processing*, Vol. 136, 2020. DOI: 10.1016/j.ymssp.2019.106523
- [10] E. Carden and P. Fanning, "Vibration based conditioning monitoring: A review", *Structural Health Monitoring*, Vol. 3, No. 4, pp. 355-377, 2004. DOI: 10.1177/1475921704047500
- [11] A. Pandey, M. Biswas, and M. Samman, "Damage detection from changes in curvature mode shapes", *Journal of Sound and Vibration*, Vol. 145, Iss. 2, pp. 321-332, 1991. DOI: 10.1016/0022-460X(91)90595-B
- [12] A. Dutta and S. Talukdar, "Damage detection in bridges using accurate modal parameters", *Finite Elements in Analysis and Design*, Vol. 40, pp. 287-304, 2004. DOI: 10.1016/S0168-874X(02)00227-5
- [13] R. Gorgin, "Damage identification technique based on mode shape analysis of beam structures", *Structures*, Vol. 27, pp. 2300-2308, 2020. DOI: 10.1016/j.istruc.2020.08.034
- [14] M. Dahak, N. Touat, and M. Kharoubi, "Damage detection in beam through change in measured frequency and undamaged curvature mode shape", *Inverse Problems in Science and Engineering*, Vol. 27, No. 2, pp. 1-26, 2018. DOI: 10.1080/17415977.2018.1442834
- [15] D. Capecchi, J. Ciambella, A. Pau, and F. Vestroni, "Damage identification in a parabolic arch by means of natural frequencies, modal shapes and curvatures", *Meccanica*, Vol. 51, No. 11, pp. 467-476, 2016. DOI: 10.1007/s11012-016-0510-3
- [16] J. W. Lee, "Crack identification method for tapered cantilever pipe-type beam using natural frequencies", *International Journal of Steel Structures*, Vol. 16, No. 2, pp. 467-476, 2016. DOI: 10.1007/s13296-016-6017-x
- [17] M. T. V. Baghmisheh, M. Peimani, M. H. Sadeghi, and M. M. Ettefagh, "Crack detection in beam-like structures using genetic algorithms", *Applied Soft Computing*, Vol. 8, Iss. 2, pp. 1150-1160, 2008. DOI: 10.1016/j.asoc.2007.10.003
- [18] S. A. Moezi, E. Zakeri, and A. Zare, "Structural single and multiple crack detection in cantilever beams using a hybrid Cuckoo-Nelder-Mead optimization method", *Mechanical Systems and Signal Processing*, Vol. 99, pp. 805-831, 2018. DOI: 10.1016/j.ymssp.2017.07.013

- [19] S. Khatir, K. Dekemele, M. Loccufier, T. Khatir, and M. A. Wahab, “Crack identification method in beam-like structures using changes in experimentally measured frequencies and particle swarm optimization”, *Comptes Rendus Mécanique*, Vol. 346, Iss. 2, pp. 110-120, 2018. DOI: 10.1016/j.crme.2017.11.008
- [20] D. T. Ta, “Structural health monitoring based on operational modal analysis”, Ph.D. thesis, University Paris-Saclay, 2022.

## NHẬN DẠNG HƯ HỎNG TRONG KẾT CẤU DẠNG DÀM THÔNG QUA SỰ THAY ĐỔI TẦN SỐ RIÊNG TƯƠNG ĐỐI

Tạ Đức Tuân<sup>1</sup>, Vũ Văn Tuấn<sup>1</sup>

<sup>1</sup>Viện Kỹ thuật công trình đặc biệt, Trường Đại học Kỹ thuật Lê Quý Đôn

**Tóm tắt:** Các phương pháp xác định hư hỏng dựa trên phân tích dao động đã được chứng minh hiệu quả trong việc quan trắc trạng thái kỹ thuật công trình. Các tham số dao động, bao gồm tần số tự nhiên và dạng dao động, đóng vai trò là các chỉ báo tổng thể về trạng thái của kết cấu. Những thay đổi của các tham số này có thể chỉ ra hư hỏng bên trong kết cấu. Bài báo đề xuất một phương pháp nâng cao để phát hiện hư hỏng thông qua sự thay đổi tần số dao động riêng. Bằng cách xác định sự thay đổi tần số giữa kết cấu còn nguyên vẹn và bị hư hỏng, có thể tính toán được, quá trình phát hiện hư hỏng trong kết cấu được thực hiện bằng cách ước lượng sai số nhỏ nhất tương ứng tại tất cả các vị trí trên kết cấu. Phương pháp này thực hiện so sánh các thay đổi tần số dao động đo được với các giá trị giải tích, đặc trưng cho sự thay đổi tần số do hư hỏng gây ra. Hiệu quả của phương pháp đề xuất được xác thực thông qua mô phỏng số và thử nghiệm trên kết cấu thực.

**Từ khóa:** Nhận dạng hư hỏng; thay đổi tần số dao động; dạng dao động.

Received: 09/04/2025; Revised: 23/12/2025; Accepted for publication: 26/12/2025

